# Mechanism study of serum extracellular nano-vesicles miR-412-3p targeting regulation of TEAD1 in promoting malignant biological behavior of sub-centimeter lung nodules

Yuxia Deng[a,1], Nishant Patel[b,1], Shuang Ding[c] and Haijun Zhang[a,*]

[a]*Department of Oncology, Zhongda Hospital, Medical School, Southeast University, Nanjing, China*
[b]*Department of Cardiothoracic Surgery, Children's Hospital of Nanjing Medical University, Nanjing, China*
[c]*Department of Oncology, Nanjing First Hospital, Nanjing Medical University, Nanjing, China*

**Abstract.**

**OBJECTIVE:** To investigate the impact and potential mechanisms of serum extracellular nano-vesicles (sEVs) miR-412-3p released from sub-centimeter lung nodules with a diameter of $\leqslant$ 10 mm on the malignant biological function of micro-nodular lung cancer (mnLC).

**METHODS:** A total of 87 participants were included and divided into a mnLC group ($n = 30$), a benign lung nodule (BLN) group ($n = 27$), and a healthy people control group ($n = 30$). Transmission electron microscopy (TEM), nanoparticle tracking analysis (NTA) and Western blot (WB) were used to measure the morphological characteristics and surface markers of sEVs. In vitro analysis, real-time quantitative polymerase chain reaction (RT-qPCR), CCK-8 cell proliferation assay, clone formation assay, Transwell, stem cell sphere-forming assay, and WB assay were conducted to verify the effect of miR-412-3p/TEAD1 signaling axis on the biological function of lung cancer cells through, respectively. Further validation was conducted using the serum sEVs of the participants.

**RESULTS:** The expression level of sEVs-miR-412-3p in the mnLC group was significantly higher than that in the BLN and healthy groups ($P < 0.01$). In lung cancer cell lines, miR-412-3p can negatively regulate the targeted gene TEAD1. The miR-412-3p/TEAD1 signaling axis is involved in promoting the EMT signaling pathway and regulating the malignant biological functions of lung cancer cell proliferation, migration, and stemness ($P < 0.05$). In addition, sEVs in the mnLC group significantly promoted lung cancer cell proliferation, migration, and stemness compared to the BLN and healthy groups, inhibited the expression of E-cadherin and TEAD1 in lung cancer cells, and promoted the expression of N-cadherin and Vimentin ($P < 0.05$).

**CONCLUSION:** sEVs-miR-412-3p could promote the biological process of EMT, and lead to the occurrence of malignant biological behavior in sub-centimeter lung nodules. This provides evidence for the miR-412-3p/TEAD1 signaling axis as a potential therapeutic target for mnLC.

Keywords: Micro-nodular lung cancer, serum extracellular nano-vesicles, miR-412-3p, transcriptional enhancer associated domain 1, epithelial mesenchymal transition

---

[1]These authors contributed equally.

*Corresponding author: Haijun Zhang, Department of Oncology, Zhongda Hospital, Medical School, Southeast University, Nanjing, 210009, China. E-mail: haijunzhang@seu.edu.cn, zhanghaijunseu@163.com.

## 1. Introduction

Lung cancer is one of the most common and poorly prognostic cancers worldwide, and also one of the most burdensome malignant tumors worldwide, seriously endangering human health [1,2]. Therefore, the early diagnosis and treatment of lung cancer are of great significance for improving the quality of life of patients and reducing mortality [3,4]. With the widespread application of low-dose spiral computed tomography (LDCT) in clinical practice, the detection rate of sub-centimeter lung nodules with a diameter of $\leqslant 10$ mm has significantly increased. However, there is still a lack of reliable non-invasive methods for distinguishing between benign and malignant. How to precisely evaluate the biological characteristics of sub-centimeter lung nodules, accurately identify micro-nodular lung cancer (mnLC) with a tumor diameter of $\leqslant 10$ mm, and move the diagnostic port of lung cancer forward is a difficult problem that urgently needs to be solved in clinical practice. Benign lung nodules (BLN) are mainly caused by pulmonary infection and inflammation, with over 80% being granulomas and a small portion possibly hamartomas (about 10%), while aneurysms and arteriovenous malformations are relatively rare [5]. About 80% of mnLC cases are primary lung cancer, a small portion are solitary metastases, and there are also a small number of carcinoids and lymphomas [6].

Serum extracellular nano-vesicles (sEVs) are extracellular vesicles secreted by cells with a diameter ranging from 30 to 150 nm, widely present in various bodily fluids [7]. After release, sEVs are absorbed by neighboring or distant cells, and their miRNAs are involved in regulating tumor immunity and microenvironment, which may further promote tumor growth, invasion, metastasis, angiogenesis, and drug resistance [8, 9,10]. miRNAs have become important biomarkers in non-invasive liquid biopsy of various tumors [11,12]. Previous studies reported that sEVs-miR-519a-3p secreted by gastric cancer cells could induce M2-like macrophage-mediated angiogenesis in the liver and promote liver metastasis [13]. In lung cancer, sEVs-miR-942 derived from M2 macrophages may promote lung cancer cell invasion and migration, as well as angiogenesis, making it a new therapeutic target for metastatic lung cancer [14]. Related fibroblasts in lung cancer tissue might promote tumor progression by releasing sEVs-miR-142-5p [15]. The above studies indicate that the enhanced proliferation, migration, and invasion ability of tumor cells involve changes in the microenvironment, and sEVs are important mediators in regulating the tumor microenvironment. In particular, sEVs-mediated functional miRNAs play an important role in mediating tumor occurrence and development. However, the biological function of sEVs miRNAs released from sub-cellular lung nodules in mnLC is currently unclear. In the preliminary research of this study, sEVs were isolated from the peripheral serum of patients with pulmonary nodules, and the expression profile of miRNAs contained in them was analyzed by sequencing. Our previous studies discovered that some sEVs miRNAs could be used as new biological detection markers to distinguish between benign and malignant pulmonary nodules [16,17], among which miR-412-3p is highly expressed in the peripheral serum of early lung cancer patients. Therefore, we will further investigate the role and mechanism of miR-412-3p in the malignant biological behavior of sub-centimeter pulmonary nodules.

## 2. Materials and methods

### 2.1. Clinical sample collection

This study collected 87 participants from the Department of Respiratory, Thoracic Surgery, and Oncology at the Affiliated Zhongda Hospital of Southeast University from January 2022 to June 2023. They were divided into an mnLC group ($n = 30$) based on postoperative pathological results, including 9 cases of adenocarcinoma in situ (AIS), 6 cases of micro-invasive adenocarcinoma (MIA), and 15 cases of invasive adenocarcinomas (IA); BLN group ($n = 27$) and healthy people control group ($n = 30$). The acquisition of all samples in this study was based on the full informed consent of patients and their families, and was approved by the Ethics Committee of Zhongda Hospital, Southeast University. The inclusion criteria include: (1) CT findings of single or multiple pulmonary nodules; (2) Nodule diameter $\leqslant 10$ mm; (3) Pathological diagnosis after biopsy or surgery. The exclusion criteria include: (1) the volume of exhaled air in the first second of maximum exhalation is less than 35%; (2) Bilateral pulmonary alveoli exceed one-third of the lung lobes; (3) Complete atelectasis; (4) Clear organic lung lesions; (5) Active tuberculosis; (6) Acute myocardial infarction grade IV and/or cardiac dysfunction occurring within 3 months; (7) Patients with hematological diseases or malignant tumors; (8) Pregnant women; (9) Those who cannot cooperate or refuse to receive treatment or screening normally; (10) Expected survival

time is less than 1 year; (11) Have a history of cancer, chronic obstructive pulmonary disease, respiratory infections, and other chronic diseases. Collect peripheral blood samples from all study subjects, isolate the supernatant, and immediately store it in liquid nitrogen for future use.

## 2.2. Purification and identification of sEVs

Referring to our previous research [16,17], 4–5 mL of peripheral blood was extracted from all participants, and sEVs were purified. Observe the morphological characteristics of sEVs using a transmission electronic microscope (TEM) (Tecnai G2 Spirit, 120 KV, Dawson Creek Drive Hillsboro, OR, USA). Evaluate the particle size distribution of sEVs through nanoparticle tracking analysis (NTA). The data was processed using a particle tracking program (Zetasizer Ver. 7.03, Malvern Instruments, Ltd, UK).

## 2.3. Cell culture

Normal lung epithelial cell line (BEAS-2B) and lung adenocarcinoma cell line (A549, NCI-1299, PC-9, and H1975) (ATCC, Virginia, USA), human renal epithelial cell line 293T (Wuhan Punosai, CL-0005). Lung adenocarcinoma cell lines were cultured in RPMI-1640 (A549, NCI-1299, PC-9) and DMEM complete medium (BEAS-2B, 293T, and H1975) containing 10% fetal bovine serum (FBS; Sigma Aldrich, St Louis, MO), 100 U/mL penicillin, and Cultivate streptomycin with a concentration of 100 $\mu$g/mL at 37$^\circ$C in an incubator containing 5% $CO_2$.

## 2.4. RT-qPCR

Total sEVs and BEAS-2B cells, as well as lung cancer A549, NCI-1299, PC-9, and H1975 cells, were extracted using Trizol LS (Invitrogen Life Technologies, MA, USA) reagent. After extraction, the total RNA concentration was measured using Nanodrop2000, and gene expression levels were quantitatively analyzed using Applied Biosystems 7500 Fast. Relative quantitative determination of each gene using the double standard curve method, with a relative expression level of 2 for each gene- $\Delta\Delta$ Ct method calculation, where, $\Delta$ Ct = target gene Ct value – internal reference gene Ct value, $\Delta\Delta$ Ct = transfection group $\Delta$ Ct – control group $\Delta$ Ct. The primer sequence (BIOLIGO, Shanghai, China) is as follows: (1) U6: F: 5′-CTCGCTTCGGCAGCACA-3′, R: 5′-AACGCTTCACGAATTTGCGT-3′; (2) miR-412-3p: F: 5′-CGCCGCTTCACCTGGTCCAC-3′, R: 5′-CAGCCACAAAAGAGCACAAT-3′; (3) $\beta$-actin: F: 5′-CACAGAGCCTCGCCTTTGCC-3′, R: 5′-ACCCAT GCCCACCAACG-3′; (4) TEAD1: F: 5′-ATGGAAAG GATGAGTGACTCTGC-3′, R: 5′TCCCACATGGTGG ATAGATAGC-3′. Select miR-412-3p low expression and high expression cell lines for subsequent experiments based on different intracellular miR-412-3p transcription levels.

## 2.5. Cell transfection

Synthesize mimics and inhibitors of miR-412-3p (synthesized by Shanghai Shenggong). When the cell fusion reaches 90%, it is passaged. Inoculate cells into a 6-well plate and culture for 24 h. When the cells fuse to 70%, intervene according to the reagent instructions. After transfection, continue to culture for 48 h and collect cells for subsequent experiments.

## 2.6. Marking of sEVs

Follow the product manual of sEVs green fluorescent labeling dye (PKH67) for subsequent operations (Shanghai Noning Biotechnology Co., Ltd.). Firstly, quantify the extracted sEVs, then add dye working solution and cover the centrifuge tube tightly. Mix well with a vortex oscillator for 1 min, then let it stand and incubate for 10 min; Add 10 mL of PBS to the incubated sEVs dye complex and mix well. Extract sEVs again using the sEVs extraction method to remove excess dye; Take 200 $\mu$L PBS resuspended precipitate is the stained sEVs. Peripheral serum-derived sEVs were labeled with PKH67-exo, and labeled sEVs were co-cultured with A549 cells in vitro. After 12 h, they were observed under a fluorescence microscope (CK40; Olympus Corporation, Tokyo, Japan).

## 2.7. CCK-8 cell viability experiment

Inoculate logarithmic growth phase cells in a 96 well plate, and transfect them when the cell growth fusion rate reaches 50%. Count 2000 cells per well, and set up 3 wells in each group. After transfection, continue to culture for 24, 48, 72, and 96 h. Add CCK-8 reagent 10 $\mu$L to each well cell. After incubating in a $CO_2$ incubator for 4 h, the absorbance value was $OD_{450\,nm}$.

## 2.8. Clone formation assay

Take each group of cells with a logarithmic growth phase, digest them with 0.25% trypsin, and blow them

into individual cells. Inoculate them on a 6-well plate with 700 cells per well, and culture in a 37°C incubator with a $CO_2$ content of 5%. Change the culture medium every three days until 21 days after cultivation, wash with PBS three times, then add 4% formaldehyde, fix for 10 min, and wash again three times. Add 1 mL of 1% crystal violet for staining for 15 min, wash three times with PBS solution, observe, take photos, and calculate the number of clones formed.

## 2.9. Transwell test

Take each group of cells in the logarithmic growth phase, digest them with 0.25% trypsin, blow them into a single cell suspension, adjust the cell count to $5 \times 10^5$ units/mL, add 100 $\mu$L cell suspension to the Transwell chamber, add 500 $\mu$L culture media to the lower chamber, the invasion experiment requires the addition of Matrigel matrix gel in advance in the upper chamber. After 36 h, clean the upper chamber with PBS, fix the cells passing through the upper chamber with 4% paraformaldehyde, stain with 1% crystal violet for 15 min, invert, and air dry. Observe counting and obtain images under an inverted microscope (200 ×, CK40; Olympus Corporation, Tokyo, Japan).

## 2.10. Stem cell sphere-forming assay

Digest and treat A549 and PC-9 lung cancer cells with 0.25% trypsin, centrifuge cell suspension at $300 \times$ g for 5 minutes, discard the supernatant, and perform cell counting with 3dGRO™ Regulate the cell concentration of spherical culture medium to achieve a concentration of $1 \times 10^6$ cells/mL. Take 10 $\mu$L cell suspension inoculated into Corning® Costar® Ultra-low adsorption porous plate, placed in a 37°C, 5% $CO_2$ incubator. After 7 days, observe the size and quantity of cells and count them (diameter > 75 $\mu$m cell sphere).

## 2.11. Double luciferase reporter gene detection

Using software (https://www.targetscan.org/vert_80/), one of the downstream target genes predicted to bind to miR-412-3p in lung cancer cells is transcriptional enhancer-associated domain 1 (TEAD1). Based on the binding sites of miR-412-3p and TEAD1, wild-type vectors (TEAD1 Wt) and mutant vectors (TEAD1 Mut) of TEAD1 were constructed. TEAD1 Wt+miR-412-3p mimics and TEAD1 Mut+miR-412-3p mimics were transfected into A549 lung cancer cells and 293T cells using liposomes, respectively. After transfection for 48 h, the detection was performed using a luciferase reporter gene detection kit. The operation steps are shown in the instructions [16].

## 2.12. Western blot

Collect transfected A549 and PC-9 cells and shake them on ice with lysis buffer for lysis. Quantify with BCA protein, separate by SDA-PVDF electrophoresis, and transfer to PVDF membrane. Seal the PVDF membrane at room temperature using 8% skim milk for 2 h. The ratio of primary antibodies: CD81 (1:1000, ab155760, Abcam), TSG101 (1:1000, ab225877, Abcam), Calnexin (1:1000, ab92573, Abcam), E-cadherin (1:10000, ab40772, Abcam), N-cadherin (1:5000, ab76011, Abcam), TEAD1 (1:1000, D3F7L, CST), $\beta$-actin (1:10000, ab8227, Abcam). Second antibody (goat anti-rabbit 1:5000, ab6721, Abcam). The primary antibody was incubated overnight on a shaking bed at 4°C, and the secondary antibody was incubated at room temperature for 2 h the next day. After washing the TBST membrane three times. ECL imaging (Tanon 5200; Shanghai, China)to detect protein bands.

## 2.13. Statistical analysis

Statistical analysis was conducted using the SPSS 20.0 (SPSS Inc., Chicago, USA) software system, and the experimental data was expressed as mean ± standard deviation (mean ± s). Use Student's t-test or one-way analysis of variance (ANOVA) to analyze the differences between groups. $P < 0.05$ indicates that the difference is statistically significant.

## 3. Results

### 3.1. The expression level of miR-412-3p in sEVs of patients with sub-centimeter pulmonary nodules

TEM intuitively confirmed the presence of sEVs of all three groups of participants, with a diameter of 40∼160 nm, elliptical in shape and varying in size, exhibiting membrane structural characteristics (Fig. 1A). The results of NTA technology show that the particle size of sEVs is mainly distributed between 30∼150 nm (Fig. 1B), accounting for 93.6% of the total, and the particle distribution coefficient is between 0.09 and 0.8. Western blot (WB) results showed that surface positive marker proteins TSG101 and CD81 were detected in sEVs isolated from the peripheral serum of mnLC, BLN, and health groups, while calnexin was not significantly expressed (Fig. 1C). The above results indicate that sEVs have been successfully obtained from the peripheral serum of all participants in this study. The
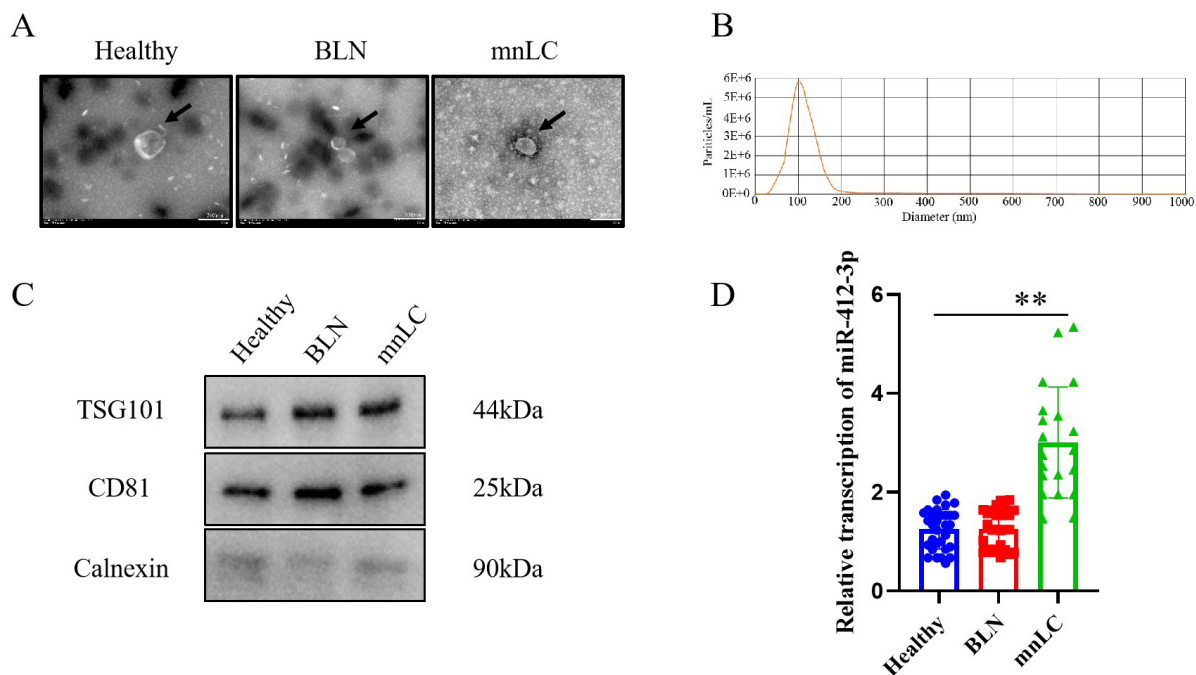
Fig. 1. Morphological characteristics and particle size distribution of sEVs in patients with sub-centimeter pulmonary nodules, as well as the expression level of miR-412-3p in sEVs. (A) TEM observation of the morphological characteristics of sEVs; (B) Evaluation of sEVs particle size distribution using nanoparticle size analysis method; (C) Surface positive markers (TSG101 and CD81) and negative markers (calnexin) protein bands of sEVs; (D) RT-qPCR was used to detect the transcription level of miR-412-3p in sEVs. $^{**}P < 0.01$, compared to the BLN and Healthy groups. All the results are representative of three independent experiments.

RT-qPCR detection results showed that compared with the BLN and healthy groups, the transcription level of miR-412-3p was highly expressed in the sEVs of the mnLC group ($P < 0.01$, Fig. 1D).

### 3.2. The effect of miR-412-3p on the viability and stemness of lung cancer cells

Research has reported that over 85% of malignant lung nodules are non-small cell lung cancer (NSCLC), with the majority being lung adenocarcinoma [18]. Therefore, lung adenocarcinoma cell lines (A549, NCI-1299, PC-9, and H1975) were selected as experimental cell lines in this experiment. The results showed that miR-412-3p was highly expressed in sEVs in the mnLC group, further exploring the impact of miR-412-3p on the malignant biological function of lung cancer cells. The RT-qPCR detection results showed that compared with normal lung cancer epithelial cells (BEAS-2B), the expression level of miR-412-3p in lung cancer cells (A549, NCI-1299, PC-9, and H1975) was significantly increased, with the highest expression level in PC-9 cells and the lowest expression level in A549 cells ($P < 0.05$, Fig. 2A). Therefore, PC-9 cells and A549 cells were selected for subsequent experimental research.

The synthesized miR-412-3p mimics and miR-412-3p inhibitor were transfected into A549 and PC-9 cells, respectively. RT-qPCR detection results showed that compared with the miR-NC mimics group, the transfected miR-412-3p mimics group significantly promoted the expression level of miR-412-3p in lung cancer A549 cells ($P < 0.01$, Fig. 2B). Compared with the miR-NC inhibitor group, the miR-412-3p inhibitor group significantly inhibited the expression level of miR-412-3p in lung cancer PC-9 cells ($P < 0.01$, Fig. 2C). The CCK-8 experiment results showed that compared with the miR-NC mimics group, the miR-412-3p mimics group significantly promoted the viability of lung cancer A549 cells ($P < 0.01$, Fig. 2D). While, compared with the miR-NC inhibitor group, transfection of miR-412-3p inhibitor significantly inhibited the viability of lung cancer PC-9 cells ($P < 0.01$, Fig. 2E).

Further cloning experiments showed that compared with the miR-NC mimics group, the miR-412-3p mimics group significantly promoted the cloning ability of lung cancer in A549 cells ($P < 0.01$, Fig. 3A). Meanwhile, compared with the miR-NC inhibitor group, transfection of the miR-412-3p inhibitor group signif-
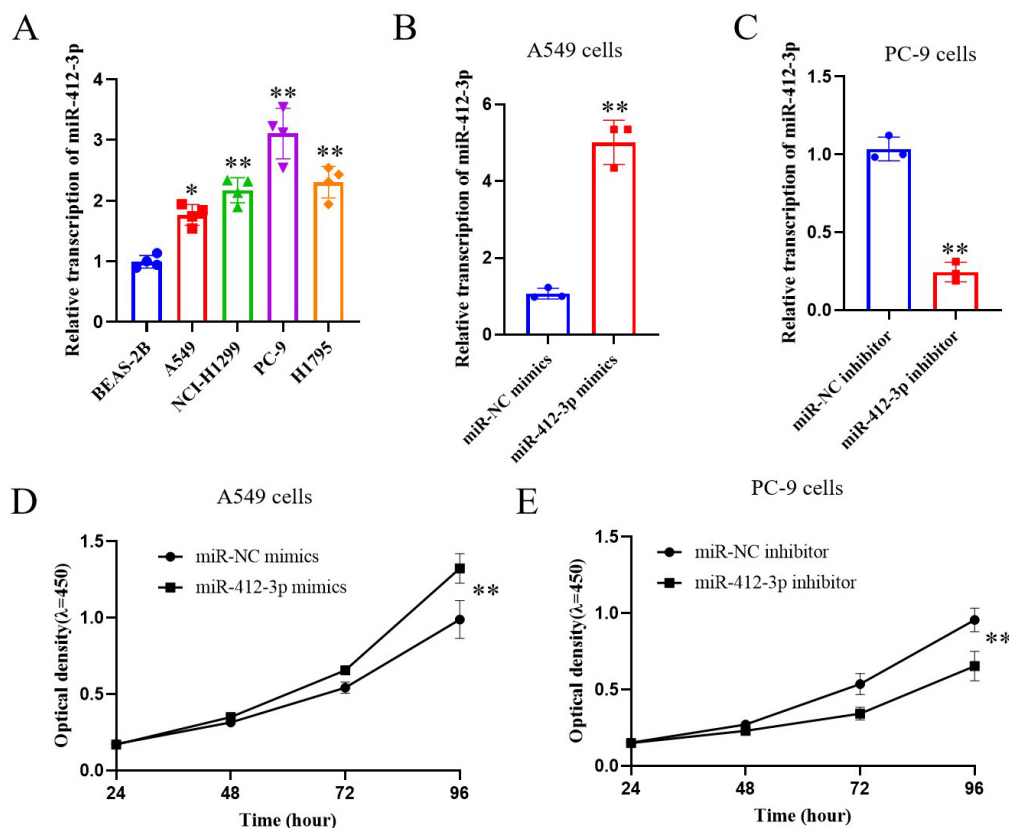
Fig. 2. miR-412-3p expression in lung cancer cells and its effect on cell viability. (A) RT-qPCR detection of miR-412-3p transcription levels in lung cancer cells; (B, C) RT-qPCR was used to detect the transcriptional levels of miR-412-3p in A549 and PC-9 cells transfected with miR-412-3p mimics and miR-412-3p inhibitor, respectively; (D, E) CCK-8 was used to detect the effect of transfection of miR-412-3p mimics and miR-412-3 inhibitor on cell viability. $^*P < 0.05$, $^{**}P < 0.01$, compared to the control group. All the results are representative of three independent experiments.

icantly inhibited the clonogenic ability of lung cancer PC-9 cells ($P < 0.01$, Fig. 3B).

The results of the stem cell sphere-forming assay showed that compared with the miR-NC mimics group, the miR-412-3p mimics group significantly promoted the stemness ability of lung cancer A549 cells ($P < 0.05$, Fig. 3C). Whereas, compared with the miR-NC inhibitor group, the miR-412-3p inhibitor group significantly inhibited the stemness ability of lung cancer PC-9 cells ($P < 0.01$, Fig. 3D). Hence, the above results signify that miR-412-3p is highly expressed in lung cancer cells and can significantly promote lung cancer cell viability, enhance their proliferation and stemness abilities.

### 3.3. The effect of miR-412-3p on the migration and invasion ability of lung cancer cells

Transwell test results showed that compared with the miR-NC mimics group, the miR-412-3p mimics group significantly promoted the migration and invasion of lung cancer A549 cells ($P < 0.01$, Fig. 4A). While, compared with the miR-NC inhibitor group, the miR-412-3p inhibitor group significantly inhibited the migration and invasion of lung cancer PC-9 cells ($P < 0.01$, Fig. 4B).

Further WB analysis showed that in A549 cells, transfection of miR-412-3p mimics significantly inhibited the expression of E-cadherin protein in lung cancer cells compared to miR-NC mimics, while promoting the expression of N-cadherin and Vimentin proteins ($P < 0.01$, Fig. 4C). In PC-9 cells with high expression of miR-412-3p, transfection of miR-412-3p inhibitor significantly promoted the expression of E-cadherin protein in lung cancer cells compared to miR-NC inhibitor, while inhibiting the expression of N-cadherin and Vimentin proteins ($P < 0.01$, Fig. 4D). All together, the results demonstrate that miR-412-3p can significantly affect the migration and invasion ability of lung cancer cells.
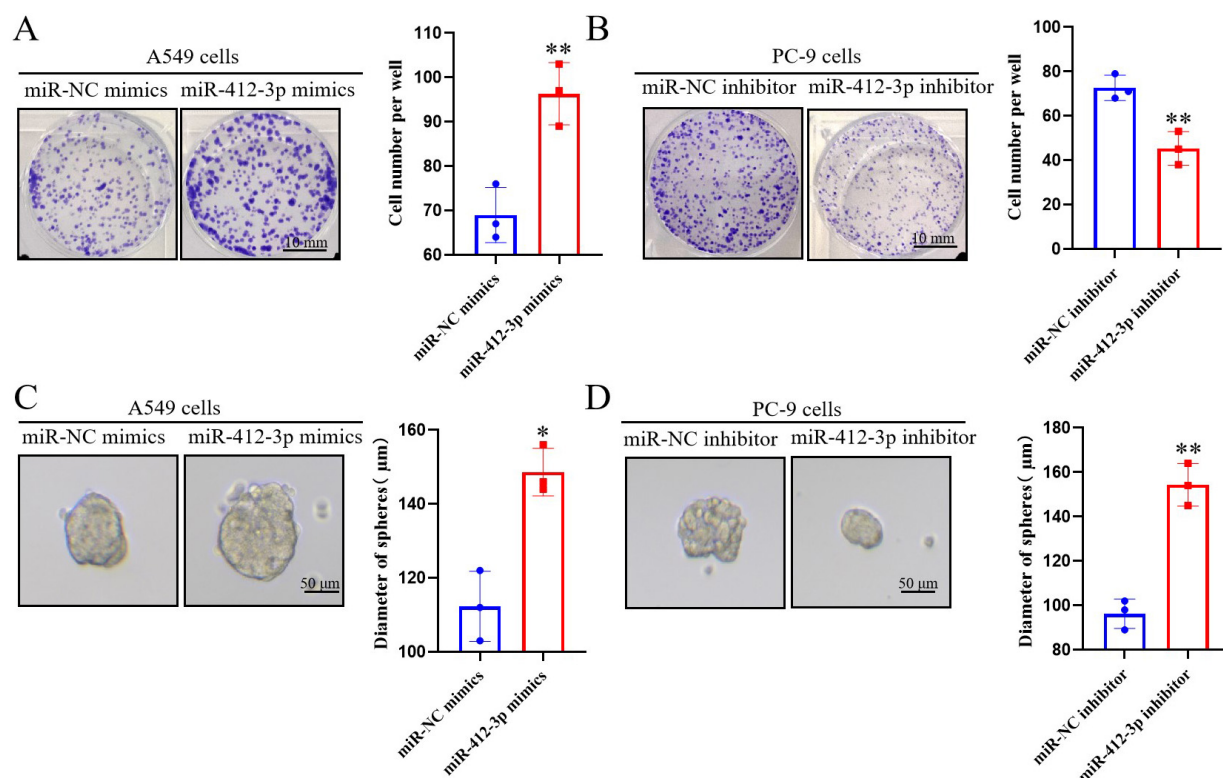
Fig. 3. The effect of miR-412-3p on clone formation and tumor stemness ability of lung cancer cells. (A, B) Plate clone formation assay to detect the effect of transfection of miR-412-3p mimics and miR-412-3p inhibitor on cell clone formation ability; (C, D) Stem cell sphere-forming assay was used to detect the effects of transfection of miR-412-3p mimics and miR-412-3p inhibitor on cell stemness ability. $^*P < 0.05$ and $^{**}P < 0.01$, compared to the control group. All the results are representative of three independent experiments.

### 3.4. The effect of miR-412-3p on TEAD1 protein in lung cancer cells

Using software (https://www.targetscan.org/vert_80/), it is predicted that one of the downstream target genes that miR-412-3p may bind to in lung cancer cells is TEAD1, and there is a binding site for miR-412-3p in the 3'UTR of its mRNA (Fig. 5A). Transfect wild-type (TEAD1 Wt) and mutant (TEAD1 Mut) luciferase reporter gene vectors into A549 cells, respectively. At the same time, co-transfect with miR-412-3p mimics and detects the activity of the luciferase reporter gene in the cells for 48 h. The results showed that in the TEAD1 Wt vector, transfection of miR-412-3p mimics significantly inhibited cell luciferase activity compared to miR-NC mimics ($P < 0.01$), while in the mutant (TEAD1 Mut) vector, there was no significant change in cell luciferase activity in the transfected miR-412-3p mimics group compared to the miR-NC mimics group (Fig. 5B).

Further validation was conducted in 293T human renal epithelial cells, and similar results were obtained. In the wild-type (TEAD1 Wt) vector, compared with

the miR-NC mimics group, the transfected miR-412-3p mimics group significantly inhibited cell luciferase activity ($P < 0.01$), while in the mutant (TEAD1 Mut) vector, compared with the blank control group (miR-NC mimics), There was no significant change in the luciferase activity of cells transfected with miR-412-3p mimics (Fig. 5C). WB analysis showed that compared with the group transfected with miR-NC mimics, miR-412-3p mimics significantly inhibited the expression of TEAD1 protein in cells ($P < 0.01$). On the contrary, compared with the miR-NC inhibitor group, the miR-412-3p inhibitor group significantly promoted the expression level of TEAD1 protein in cells ($P < 0.01$) (Fig. 5D–E). Therefore, the results suggest that miR-412-3p can bind to the downstream target gene TEAD1 and affect its expression in lung cancer cells.

### 3.5. MiR-412-3p affects the proliferation and migration ability of lung cancer cells by regulating the target gene TEAD1

Next, we will further investigate whether miR-412-3p affects the proliferation and migration ability of
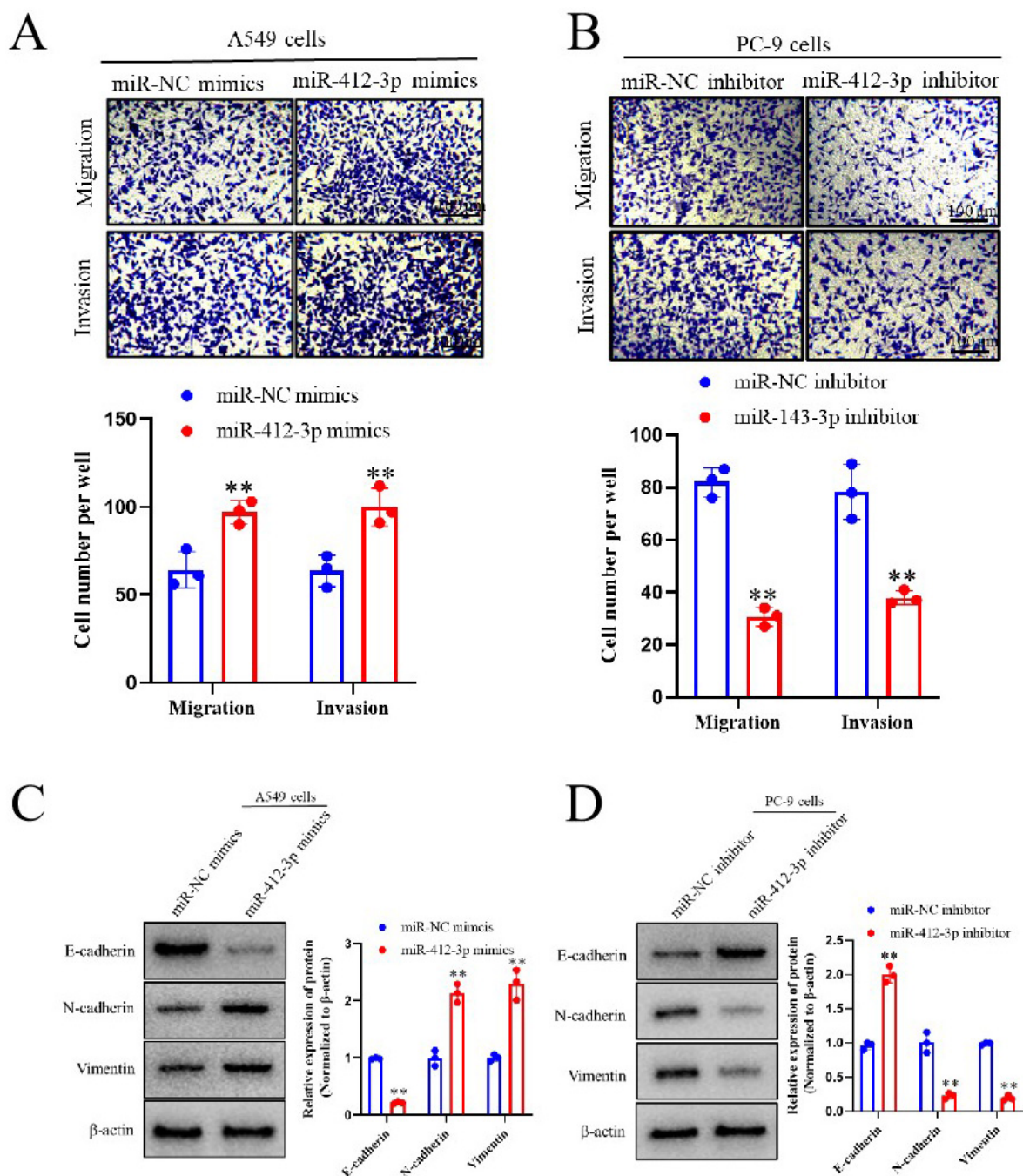
Fig. 4. The effect of miR-412-3p on the migration and invasion ability and related proteins in lung cancer cells. (A, B) Transwell assay was used to detect the effect of overexpression of miR-412-3p on the migration and invasion ability of lung cancer A549 cells (A) and PC-9 cells (B); (C, D) The effect of miR-412-3p on the expression of migration and invasion related proteins in lung cancer A549 cells (C) and PC-9 cells (D). $^{*}P < 0.05$ and $^{**}P < 0.01$, compared to the control group. All the results are representative of three independent experiments.

lung cancer cells by regulating TEAD1. Based on the above research results, it can be inferred that miR-412-3p negatively regulates the expression of TEAD1 in lung cancer cells. To further validate this inference, the constructed blank vector (pcDNA-NC) and overexpressing TEAD1 vector (pcDNA-TEAD1) were transfected into lung cancer cell A549 cells, respectively, and miR-412-3p mimics were co-transfected. The re-
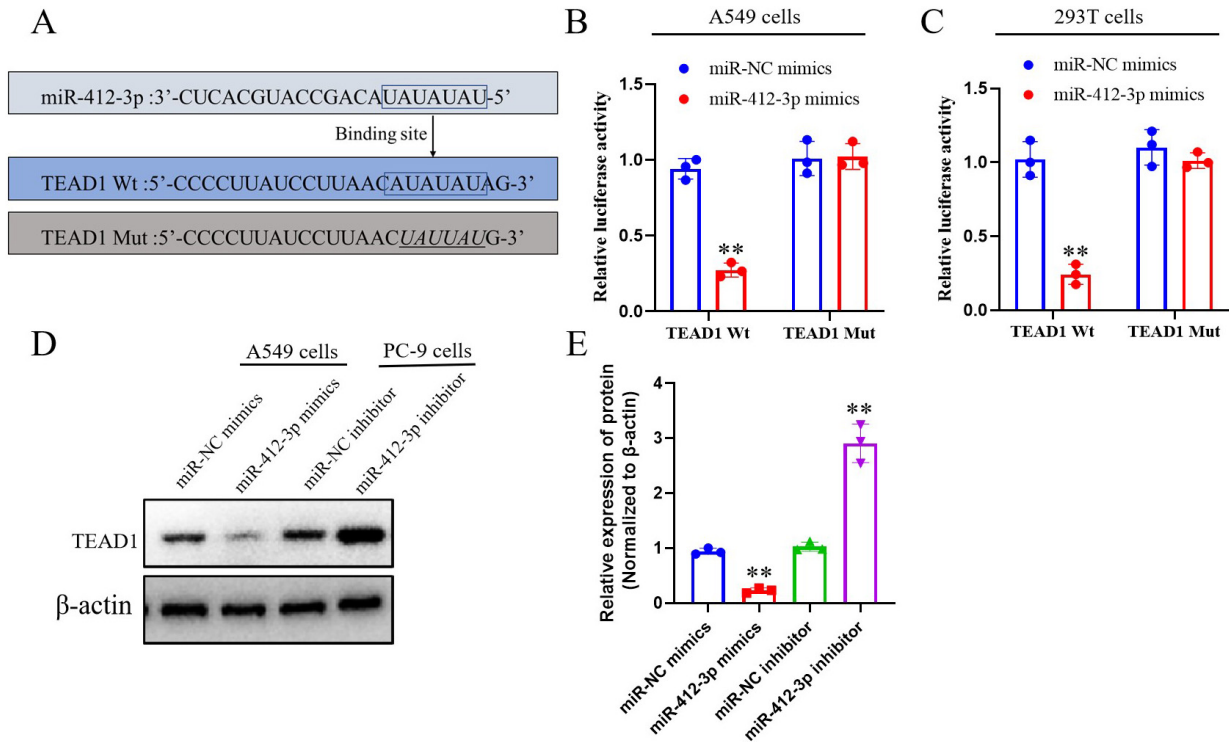
Fig. 5. The effect of miR-412-3p on downstream target gene transcriptional enhancer associated domain proteins in lung cancer cells. (A) Design luciferase reporter gene vectors for wild-type (TEAD1 Wt) and mutant (TEAD1 Mut), and analyze the binding sites of miR-412-3p to TEAD1; (B, C) Detection of cell luciferase activity of miR-412-3p binding to TEAD1 using luciferase reporter gene in A549 and 293T cells; (D) Western blot was used to detect the effects of miR-412-3p mimics and miR-412-3p inhibitor transfection on the expression of TEAD1 in lung cancer cells; (E) Statistical analysis of the expression level of TEAD1 protein in Figure D. $*P < 0.05$ and $**P < 0.01$, compared to the control group. All the results are representative of three independent experiments.

sults of clone formation and migration experiments showed that compared with miR-NC mimics, transfection of miR-412-3p mimics significantly promoted the clone formation ($P = 0.009$) and migration ability of lung cancer cells ($P = 0.002$). In the miR-412-3p mimics group, after transfection with blank vector group (pcDNA-NC) and overexpressing TEAD1 vector group (pcDNA-TEAD1), compared with the miR-412-3p mimics+pcDNA-NC group, the number of cell clones formed ($P = 0.0249$, Fig. 6A–B) and migration ability significantly decreased ($P = 0.0076$, Fig. 6C–D) in the miR-412-3p mimics+overexpressing TEAD1 group. Thus, the results showed that overexpression of TEAD1 (pcDNA-TEAD1) significantly inhibited the promoting effect of miR-412-3p mimics on the clonal formation and migration ability of lung cancer cells.

### 3.6. sEVs promote the proliferation, stemness, and migration ability of lung cancer cells

Select A549 cells with the lowest expression level of miR-412-3p from lung cancer cells (A549, NCI-1299,

PC-9, and H1975) as the experimental cell model for detecting the effect of sEVs on lung cancer cells. Separate sEVs from the mnLC group, BLN group, and healthy group, and incubate them with A549 cells respectively. The changes in sEVs uptake by A549 cells can be clearly observed using immunofluorescence, and the results show that green fluorescent labeled sEVs (PKH67) can enter A549 cells (Fig. 7A). Further cellular biology functional experiments showed that compared with the sEVs of the BLN and healthy people groups, sEVs in the mnLC group significantly promoted the ability of lung cancer cells to form clones, dry and migrate ($P < 0.01$, Fig. 7B~D).

Further WB analysis showed that compared with the sEVs of the BLN and health groups, the sEVs of the mnLC group significantly inhibited the expression of E-cadherin and TEAD1 proteins in lung cancer cells, while promoting the expression of N-cadherin and Vimentin proteins ($P < 0.01$, Fig. 7E~H).

In summary, the results of this study found that sEVs-miR-412-3p was highly expressed in the serum of mnLC patients, suggesting that miR-412-3p may play
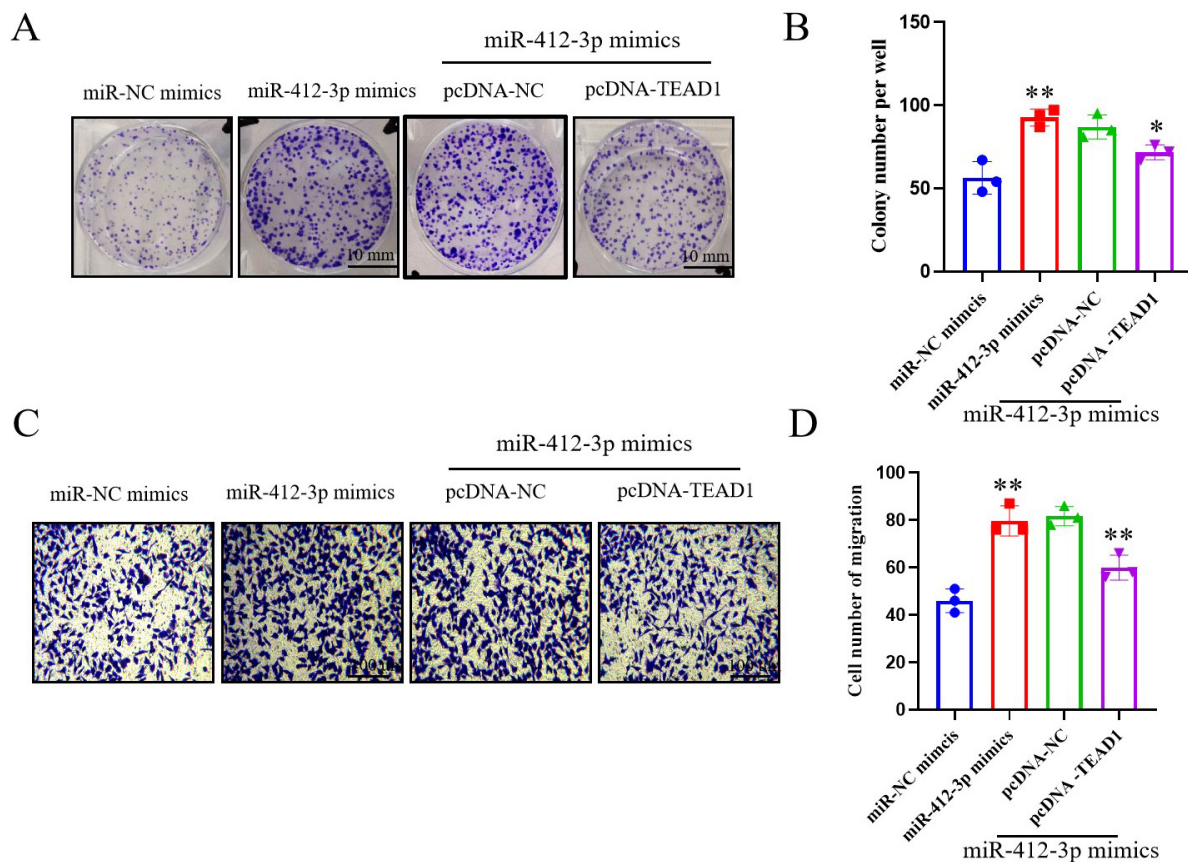
Fig. 6. The effect of miR-412-3p on the proliferation and migration ability of lung cancer cells by regulating TEAD1. In the experiment, miR-412-3p mimics group and miR-NC mimics were established; Based on the miR-412-3p mimics group, a transfer with pcDNA-NC and pcDNA-TEAD1 were established. (A) The clone formation experiment detected that miR-412-3p affects the proliferation ability of lung cancer cells by regulating TEAD1; (B) Statistical analysis of clone formation experimental bar charts; (C) Transwell migration assay detected that miR-412-3p affects the migration ability of lung cancer cells by regulating TEAD1; (D) Statistical analysis of Transwell test cell migration bar chart. $^*P < 0.05$, $^{**}P < 0.01$, compared to the control group. All the results are representative of three independent experiments.

an important role in the occurrence of early lung cancer. The results of in vitro cell experiments confirmed our hypothesis: miR-412-3p targeted regulation of the TEAD1 signaling pathway plays an important role in early lung cancer (Fig. 8). The high expression of miR-412-3p in lung cancer cells promotes the expression of N-cadherin and Vimentin proteins, inhibits the expression of E-cadherin proteins, induces the epithelial-mesenchymal transition (EMT) process in lung cancer cells, and enhances their proliferation, stemness, and migration abilities by inhibiting TEAD1.

## 4.  Discussion

Lung cancer is one of the most widely distributed malignant tumors worldwide, with an age-standardized 5-year survival rate of only 10% to 20% [19]. The EMT process is related to tumor occurrence and development, and tumor cells enhance their migration and invasion abilities through the EMT process [20]. During the process, EMT not only manifests as changes in cellular morphology, but is also accompanied by changes in related molecular markers such as E-cadherin, N-cadherin, and Vimentin [21]. Early lung cancer screening for high-risk populations has become an important link in reducing lung cancer mortality and reducing the burden of lung cancer in various countries. With the widespread application of LDCT in early lung cancer screening, the detection rate of sub-centimeter lung nodules with a diameter of ⩽ 10 mm has significantly increased. The fear and concern among the public about the malignant transformation of sub-centimeter pulmonary nodules have led to the occurrence of over diagnosis and over treatment of sub-centimeter pulmonary nodules. Therefore, it is particularly important and ur-
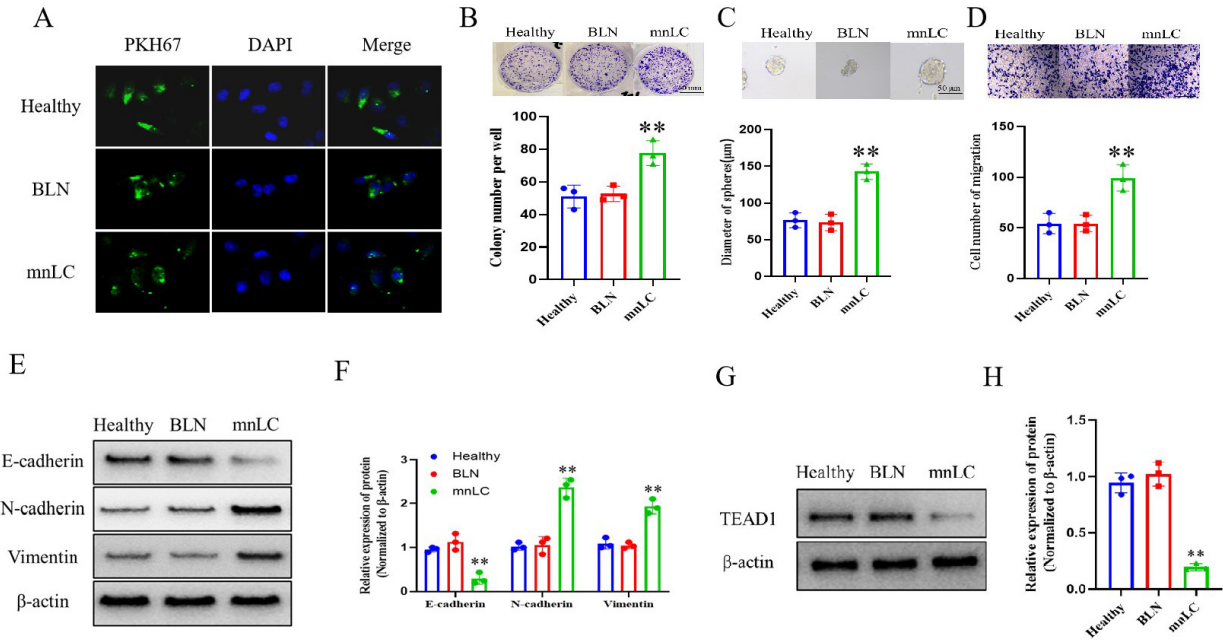
Fig. 7. sEVs enhance the proliferation, stemness, migration ability, invasion and TEAD1 related protiens of lung cancer A549 cells. (A) Immunofluorescence observation of the localization of green fluorescent labeled sEVs (PKH67) after incubation with lung cancer cells; (B) The effect of adding sEVs on cell clone formation ability in clone formation detection; (C) The effect of adding sEVs on cell stemness ability was detected through Stem cell sphere-forming assay; (D) Transwell assay was used to detect the effect of adding sEVs on cell migration ability. (E) Representative lung cancer cell A549 invasion related protein band diagram; (F) Histogram of expression of invasion related proteins in A549 lung cancer cells; (G) Intracellular TEAD1 protein band diagram of representative lung cancer cell A549; (H) Histogram of TEAD1 protein expression in A549 lung cancer cells. $^{**}P < 0.01$, compared to the BLN and Healthy groups. All the results are representative of three independent experiments.
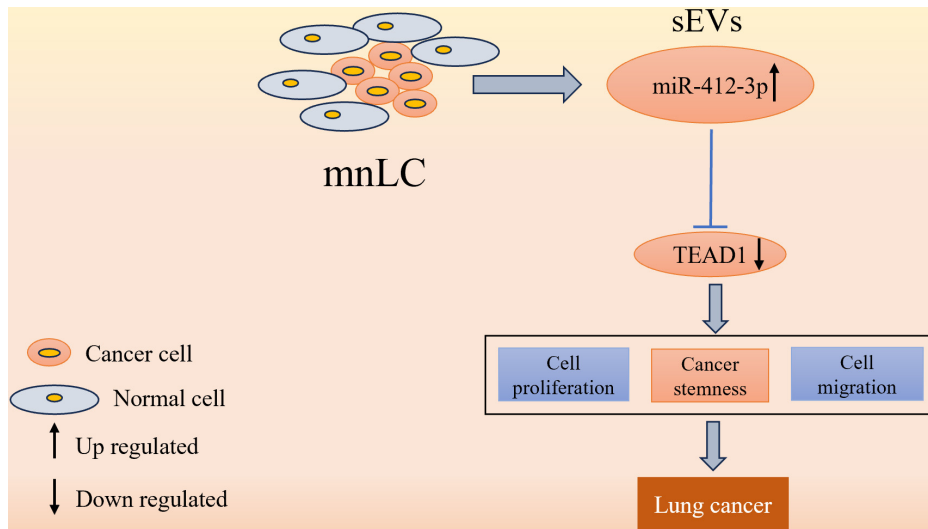


Fig. 8. Schematic diagram of sEVs miR-412-3p promoting early lung cancer development through targeted regulation of TEAD1 signaling axis in micro-nodular lung cancer.

gent to seek early biomarkers that can effectively distinguish benign sub-centimeter pulmonary nodules from mnLC. This study found that miR-412-3p is highly ex-

pressed in sEVs of mnLC patients. The results of cell biology functional experiments suggest that miR-412-3p can significantly affect the proliferation, stemness,

migration, and invasion ability of lung cancer cells, and miR-412-3p can target downstream gene TEAD1 to inhibit TEAD1 expression; On the contrary, overexpression of TEAD1 can significantly block the function of miR-412-3p oncogenes. Therefore, the miR-412-3p/TEAD1 signaling axis might serve as a potential therapeutic target for blocking the malignant biological behavior of mnLC.

The sEVs are important mediators of intercellular communication, carrying abundant miRNAs and proteins that play important roles in information transmission between tumor cells and their microenvironment. Meanwhile, sEVs participate in regulating tumor cell proliferation, stemness, migration, and invasion ability, and can serve as a potential biomarker for early diagnosis of tumors [22,23,24]. Previous research reported fibrinogen $\beta$ and fibrinogen $\gamma$ from serum sEVs as potential biomarkers for distinguishing benign from malignant pulmonary nodules [25]. Proteomic analysis of sEVs in distinguishing benign and malignant pulmonary nodules revealed 33 differentially expressed proteins, of which 12 proteins were only expressed in the benign nodule group and 9 proteins were only expressed in the malignant nodule group [26]. In addition, the miR-21/Let-7a ratio in sEVs can be used as a biomarker to distinguish NSCLC from benign lung diseases [27]. Preliminary studies have reported that serum miRNAs, carcinoembryonic antigen (CEA), cytokeratin 19 fragment (CYFRA21-1), and imaging and clinical features have been used to differentiate between benign and malignant pulmonary nodules. Patients with malignant pulmonary nodules have significantly higher levels of serum miR-21-5p and miR-574-5p compared to patients with benign nodules, making them potential serum biomarkers. The predictive model constructed by them can shorten the diagnostic time of malignant nodules [28]. The above results indicate that miRNAs in serum can serve as a potential diagnostic marker for distinguishing between benign and malignant pulmonary nodules. This study found high expression of miR-412-3p in sEVs of mnLC patients, suggesting that miR-412-3p would serve as a potential biomarker for distinguishing benign and malignant sub-centimeter pulmonary nodules.

miR-412-3p is a newly identified class of non-coding miRNAs that are involved in regulating the occurrence and development of colorectal and renal cancer [29,30]. In colorectal cancer, miR-412-3p acts as a pro-oncogene and promotes tumor progression by negatively regulating the expression of MYL9 which may mediate canceration through the TGF$\beta$1/PI3K/AKT axis [30,31].

miR-412-3p could also promote the proliferation and invasion ability of renal cancer cells by negatively regulating the expression of PCDH7 [29] which can mediate tumorigenesis by MAPK signaling [32]. In our study, TEAD1 is also a known target gene of miR-412-3p, it is plausible that miR-412-3p interacts with multiple pathways to influence tumor progression. The above research results help underline the multifaceted role of miR-412-3p in cancer biology, suggesting that it may regulate a network of genes and pathways to promote tumorigenesis and cancer progression.

The results of this study's cell function experiment showed that transfection of miR-412-3p mimics significantly promoted the proliferation, stemness, migration, and invasion ability of lung cancer cells, while transfection of miR-412-3p inhibitor significantly inhibited the biological functions of lung cancer cells mentioned above, suggesting that miR-412-3p, as an oncogenic gene, significantly promote the progression of lung cancer. Therefore, we speculate that sEVs-miR-412-3p released by mnLC may significantly promote the proliferation of lung cancer cells, enhance the stem cell characteristics of lung cancer cells themselves, and enhance their ability to invade and migrate surrounding tissues. Biological information software prediction and luciferase reporter gene results show that one of the target genes of miR-412-3p is TEAD1, and miR-412-3p binds and negatively regulates the expression of TEAD1. Previous studies have reported that TEAD1 could regulate cell proliferation and stem cell function [33,34], and reducing TEAD1 expression should significantly affect Hippo, Wnt, and TGF-$\beta$. The epidermal growth factor receptor (EGFR) pathway plays an important role in tumor progression, metastasis, tumor metabolism, immunity, and drug resistance [35]. Meanwhile, TEAD1 plays an important role in the progression of malignant tumors and can serve as a biomarker related to the survival prognosis of tumor patients [36]. As a tumor suppressor gene, the decreased expression of TEAD1 can promote the activation of intracellular procancer signaling pathways, leading to the occurrence and development of tumors. These functions have also been confirmed by in vitro experiments in this study. Overexpression of TEAD1 can significantly block the promoting effect of miR-412-3p on the proliferation and migration of lung cancer cells. The results of this study confirm our hypothesis that miR-412-3p exerts its biological function by negatively regulating TEAD1. The sEVs with high expression of miR-412-3p in peripheral serum are ingested by lung cancer cells, which in turn inhibit the expression of E-cadherin and TEAD1,

promote the expression of N-cadherin and Vimentin, and improve the proliferation, stemness, and migration ability of lung cancer cells. Nevertheless, future studies are warranted to further validate the in-depth role and mechanism of serum sEVs-mediated miR-412-3p in lung cancer.

In summary, this study constraints that miR-412-3p targets negative regulation of TEAD1 and plays an important role in the malignant proliferation, stemness, invasion, and migration ability, as well as EMT process of lung cancer cells, exhibiting a progression in promoting the malignant biological behavior of sub-centimeter lung nodules. Therefore, drugs or inhibitors targeting the miR-412-3p/TEAD1 signaling axis may be an effective target for inhibiting the malignant biological behavior of mnLC in the future.

## Acknowledgments

## Funding

## Author contributions

Conception: YD, NP, HZ.
Interpretation or analysis of data: YD, NP, SD, HZ.
Preparation of the manuscript: YD, NP, SD, HZ.
Revision for important intellectual content: YD, NP, HZ.
Supervision: HZ.

## Conflict of interest

Nothing to declare.

## References

[1]  F. Abu Rous, E.K. Singhi, A. Sridhar, M.S. Faisal and A. Desai, Lung Cancer Treatment Advances in 2022, *Cancer Invest* **41** (2023), 12–24.

[2]  S.J. Adams, E. Stone, D.R. Baldwin, R. Vliegenthart, P. Lee and F.J. Fintelmann, Lung cancer screening, *Lancet* **401** (2023), 390–408.

[3]  S. Huang, J. Yang, N. Shen, Q. Xu and Q. Zhao, Artificial intelligence in lung cancer diagnosis and prognosis: Current application and future perspective, *Semin Cancer Biol* **89** (2023), 30–37.

[4]  P. Li, S. Liu, L. Du, G. Mohseni, Y. Zhang and C. Wang, Liquid biopsies based on DNA methylation as biomarkers for the detection and prognosis of lung cancer, *Clin Epigenetics* **14** (2022), 118.

[5]  Z. Wu, F. Wang, W. Cao, C. Qin, X. Dong, Z. Yang, Y. Zheng, Z. Luo, L. Zhao, Y. Yu, Y. Xu, J. Li, W. Tang, S. Shen, N. Wu, F. Tan, N. Li and J. He, Lung cancer risk prediction models based on pulmonary nodules: A systematic review, *Thorac Cancer* **13** (2022), 664–677.

[6]  T.J. Kim, C.H. Kim, H.Y. Lee, M.J. Chung, S.H. Shin, K.J. Lee and K.S. Lee, Management of incidental pulmonary nodules: current strategies and future perspectives, *Expert Rev Respir Med* **14** (2020), 173–194.

[7]  R. Kalluri and V.S. LeBleu, The biology, function, and biomedical applications of exosomes, *Science*, **367** (2020), eaau6977.

[8]  R. Isaac, F.C.G. Reis, W. Ying and J.M. Olefsky, Exosomes as mediators of intercellular crosstalk in metabolism, *Cell Metab* **33** (2021), 1744–1762.

[9]  B. Li, Y. Cao, M. Sun and H. Feng, Expression, regulation, and function of exosome-derived miRNAs in cancer progression and therapy, *Faseb J* **35** (2021), e21916.

[10]  J. Chen, F. Cao, Y. Cao, S. Wei, X. Zhu and W. Xing, Targeted therapy of lung adenocarcinoma by the nanoplatform based on milk exosomes loaded with paclitaxel, *J Biomed Nanotechnol* **18** (2022), 1075–1083.

[11]  V.C. Kok and C.C. Yu, Cancer-Derived Exosomes: Their Role in Cancer Biology and Biomarker Development, *Int J Nanomedicine* **15** (2020), 8019–8036.

[12]  F.G. Kugeratski, K. Hodge, S. Lilla, K.M. McAndrews, X. Zhou, R.F. Hwang, S. Zanivan and R. Kalluri, Quantitative proteomics identifies the core proteome of exosomes with syntenin-1 as the highest abundant protein and a putative universal biomarker, *Nat Cell Biol* **23** (2021), 631–641.

[13]  S. Qiu, L. Xie, C. Lu, C. Gu, Y. Xia, J. Lv, Z. Xuan, L. Fang, J. Yang, L. Zhang, Z. Li, W. Wang, H. Xu, B. Li and Z. Xu, Gastric cancer-derived exosomal miR-519a-3p promotes liver metastasis by inducing intrahepatic M2-like macrophage-mediated angiogenesis, *J Exp Clin Cancer Res* **41** (2022), 296.

[14]  K. Wei, Z. Ma, F. Yang, X. Zhao, W. Jiang, C. Pan, Z. Li, X. Pan, Z. He, J. Xu, W. Wu, Y. Xia and L. Chen, M2 macrophage-derived exosomes promote lung adenocarcinoma progression by delivering miR-942, *Cancer Lett* **526** (2022), 205–216.

[15]  Y. Jiang, K. Wang, X. Lu, Y. Wang and J. Chen, Cancer-associated fibroblasts-derived exosomes promote lung cancer progression by OIP5-AS1/ miR-142-5p/ PD-L1 axis, *Mol Immunol* **140** (2021), 47–58.

[16]  Y. Deng, R. Xue, N. Patel, W. Xu and H. Zhang, Serum extracellular nano-vesicles miR-153-3p to Identify micronodular lung cancer from sub-centimeter lung nodules, *J Biomed Nanotechnol* **18** (2022), 705–717.

[17]  N. Patel, W. Xu, Y. Deng, J. Jin and H. Zhang, Cross-scale integration of nano-sized extracellular vesicle-based biomarker and radiomics features for predicting suspected sub-solid pulmonary nodules, *J Biomed Nanotechnol* **17** (2021), 1109–1122.

[18]  Y. Su, H.B. Fang and F. Jiang, An epigenetic classifier for early stage lung cancer, *Clin Epigenetics* **10** (2018), 68.

[19]  C. Allemani, T. Matsuda, V. Di Carlo, R. Harewood, M. Matz, M. Nikšić, A. Bonaventure, M. Valkov, C.J. Johnson, J. Estève, O.J. Ogunbiyi, E.S.G. Azevedo, W.Q. Chen, S. Eser, G. Engholm, C.A. Stiller, A. Monnereau, R.R. Woods, O. Visser, G.H. Lim, J. Aitken, H.K. Weir and M.P. Coleman, Global surveillance of trends in cancer survival 2000-14 (CONCORD-3): analysis of individual records for 37 513 025 patients diagnosed with one of 18 cancers from 322 population-based

registries in 71 countries, *Lancet* **391** (2018), 1023–1075.

[20]  A. Dongre and R.A. Weinberg, New insights into the mechanisms of epithelial-mesenchymal transition and implications for cancer, *Nat Rev Mol Cell Biol* **20** (2019), 69–84.

[21]  R. Kalluri and R.A. Weinberg, The basics of epithelial-mesenchymal transition, *J Clin Invest* **119** (2009), 1420–1428.

[22]  Q.F. Han, W.J. Li, K.S. Hu, J. Gao, W.L. Zhai, J.H. Yang and S.J. Zhang, Exosome biogenesis: machinery, regulation, and therapeutic implications in cancer, *Mol Cancer* **21** (2022), 207.

[23]  F. Man, J. Wang and R. Lu, Techniques and applications of animal- and plant-derived exosome-based drug delivery system, *J Biomed Nanotechnol* **16** (2020), 1543–1569.

[24]  D. He, X. Xu, L. Li, C. Chen, K. Gong, Q. Guo, F. Liu, Y. Wang, Y. Duan and H. Li, Functional exosome-mediated delivery of triptolide endowed with targeting properties as chemotherapy carriers for ovarian carcinoma, *J Biomed Nanotechnol* **17** (2021), 426–438.

[25]  M. Kuang, Y. Peng, X. Tao, Z. Zhou, H. Mao, L. Zhuge, Y. Sun and H. Zhang, FGB and FGG derived from plasma exosomes as potential biomarkers to distinguish benign from malignant pulmonary nodules, *Clin Exp Med* **19** (2019), 557–564.

[26]  M. Kuang, X. Tao, Y. Peng, W. Zhang, Y. Pan, L. Cheng, C. Yuan, Y. Zhao, H. Mao, L. Zhuge, Z. Zhou, H. Chen and Y. Sun, Proteomic analysis of plasma exosomes to differentiate malignant from benign pulmonary nodules, *Clin Proteomics* **16** (2019), 5.

[27]  G. Yang, T. Wang, X. Qu, S. Chen, Z. Han, S. Chen, M. Chen, J. Lin, S. Yu, L. Gao, K. Peng and M. Kang, Exosomal miR-21/Let-7a ratio distinguishes non-small cell lung cancer from benign pulmonary diseases, *Asia Pac J Clin Oncol* **16** (2020), 280–286.

[28]  X. Li, Q. Zhang, X. Jin and L. Cao, Combining serum miRNAs, CEA, and CYFRA21-1 with imaging and clinical features to distinguish benign and malignant pulmonary nodules: a pilot study: Xianfeng Li, et al.: Combining biomarker, imaging, and clinical features to distinguish pulmonary nodules, *World J Surg Oncol* **15** (2017), 107.

[29]  Y. Wang, Y. Zhang, X. Su, Q. Qiu, Y. Yuan, C. Weng, S. Zou, Y. Tian, W. Han, P. Liu, X. Guo, J. Mao, X. Fu, P. Wang and

W. Lin, Circular RNA circDVL1 inhibits clear cell renal cell carcinoma progression through the miR-412-3p/PCDH7 axis, *Int J Biol Sci* **18** (2022), 1491–1507.

[30]  K. Zhu, Y. Wang, L. Liu, S. Li and W. Yu, Long non-coding RNA MBNL1-AS1 regulates proliferation, migration, and invasion of cancer stem cells in colon cancer by interacting with MYL9 via sponging microRNA-412-3p, *Clin Res Hepatol Gastroenterol* **44** (2020), 101–114.

[31]  S. Deng, D. Cheng, J. Wang, J. Gu, Y. Xue, Z. Jiang, L. Qin, F. Mao, Y. Cao and K. Cai, MYL9 expressed in cancer-associated fibroblasts regulate the immune microenvironment of colorectal cancer and promotes tumor progression in an autocrine manner, *J Exp Clin Cancer Res* **42** (2023), 294.

[32]  X. Zhou, B.L. Updegraff, Y. Guo, M. Peyton, L. Girard, J.E. Larsen, X.J. Xie, Y. Zhou, T.H. Hwang, Y. Xie, J. Rodriguez-Canales, P. Villalobos, C. Behrens, Wistuba, II, J.D. Minna and K.A. O'Donnell, PROTOCADHERIN 7 Acts through SET and PP2A to Potentiate MAPK Signaling by EGFR and KRAS during Lung Tumorigenesis, *Cancer Res* **77** (2017), 187–197.

[33]  H.D. Huh, D.H. Kim, H.S. Jeong and H.W. Park, Regulation of TEAD transcription factors in cancer biology, *Cells* **8** (2019), 600.

[34]  A.V. Pobbati, R. Kumar, B.P. Rubin and W. Hong, Therapeutic targeting of TEAD transcription factors in cancer, *Trends Biochem Sci* **48** (2023), 450–462.

[35]  L. Currey, S. Thor and M. Piper, TEAD family transcription factors in development and disease, *Development* **148** (2021), dev196675.

[36]  T.J. Hagenbeek, J.R. Zbieg, M. Hafner, R. Mroue, J.A. Lacap, N.M. Sodir, C.L. Noland, S. Afghani, A. Kishore, K.P. Bhat, X. Yao, S. Schmidt, S. Clausen, M. Steffek, W. Lee, P. Beroza, S. Martin, E. Lin, R. Fong, P. Di Lello, M.H. Kubala, M.N. Yang, J.T. Lau, E. Chan, A. Arrazate, L. An, E. Levy, M.N. Lorenzo, H.J. Lee, T.H. Pham, Z. Modrusan, R. Zang, Y.C. Chen, M. Kabza, M. Ahmed, J. Li, M.T. Chang, D. Maddalo, M. Evangelista, X. Ye, J.J. Crawford and A. Dey, An allosteric pan-TEAD inhibitor blocks oncogenic YAP/TAZ signaling and overcomes KRAS G12C inhibitor resistance, *Nat Cancer* **4** (2023), 812–828.